CD44, TLR4, TREM-1/DAP12 in renal injury, inflammation and fibrosis

Rampanelli, E.

Publication date
2014

5

CD44v3-v10 reduces the pro-fibrotic effects of TGF-β1 and attenuates tubular injury in the early stage of chronic obstructive nephropathy

Elena Rampanelli[1]
Kasper Rouschop[2]
Gwendoline J. D. Teske[1]
Nike Claessen[1]
Jaklien C. Leemans[1]
Sandrine Florquin[1,3]

[1]Department of Pathology, Academic Medical Center, University of Amsterdam, Amsterdam, The Netherlands.
[2]Maastricht Radiation Oncology (Maastro), GROW School for Oncology and Developmental Biology, University of Maastricht, Maastricht, The Netherlands.
[3]Department of Pathology, Radboud University Nijmegen Center, Nijmegen, The Netherlands.

American Journal of Physiology - Renal Physiology, 305: F1445–F1454, 2013.

Abstract

CD44 family members are cell surface glycoproteins, which are expressed on tubular epithelial cells (TEC) solely upon kidney injury and are involved in renal fibrosis development. Renal interstitial fibrosis is the final manifestation of chronic kidney diseases and is regulated by a complex network of cytokines, including the pro-fibrotic factor TGF-β1 and the two anti-fibrotic cytokines BMP-7 and HGF. The present study investigates the potential role of CD44 standard (CD44s) and CD44v3-v10 (CD44v3) isoforms as modulators of the balance between TGF-β1 and HGF/BMP-7. CD44s is the shortest and most common isoform. CD44v3-v10 (CD44v3) has heparan sulfate moieties, which enable the binding to HGF/BMP-7, and hence, might exert reno-protective effects.

Using transgenic mice overexpressing either CD44s or CD44v3 specifically on proximal TEC, we found that in vitro the overexpression of CD44v3 on primary TEC renders cells less susceptible to TGF-β1 pro-fibrotic actions and more sensitive to BMP-7 and HGF in comparison to TEC overexpressing CD44s. One day after unilateral ureteric obstruction, obstructed kidneys from CD44v3 transgenic mice showed less tubular damage and myofibroblasts accumulation, which was associated with decreased TGF-β1 signaling and increased BMP-7 synthesis and signaling compared to kidneys from WT and CD44s transgenic mice. These data suggest that CD44v3 plays a renoprotective role in early stage of chronic obstructive nephropathy.

Introduction

Progressive renal fibrosis is the final common manifestation of various chronic kidney diseases (CKD) leading to irreversible loss of nephrons and end-stage renal failure[36] Myofibroblasts and tubular epithelial cells (TEC) are key players in kidney fibrosis:[39] myofibroblasts are the major producers of extracellular matrix (ECM);[58] whereas TEC may lose expression of cell adhesion molecules, produce cytokines and undergo epithelial-mesenchymal transition (EMT).[15,23,36] Fibroblast activation and proliferation is triggered by local secreted fibrogenic cytokines such as transforming growth factor-β1 (TGF-β1),[49] connective tissue growth factor (CTGF),[59] and monocyte chemotactic protein-1 (MCP-1).[35] Fibroblast-activation and collagen deposition are antagonized by hepatocyte growth factor (HGF)[10] and bone morphogenic protein-7 (BMP-7).[63]

The transmembrane glycoprotein CD44 is one of these factors that might orchestrate the balance between pro- and anti-fibrotic molecules.[13] CD44 is a widely expressed cell adhesion receptor encoded by a gene of 19 exons, of which 10 are alternatively spliced exons within the extracellular domain that can generate different isoforms.[51] CD44 family members function as co-receptors or/and as specialized platforms for growth factors, chemokines, components of the ECM and matrix metalloproteases (MMP).[42] CD44 can interact with TGF-β receptor type I ,[5] and recruit to cell surface MMP-9, which in turn is able to cleave pro-TGF-β1 into its active form.[61] CD44 standard (CD44s) is the smallest isoform lacking all variable exons and the most abundant member found on many different cell types.[42] Isoforms containing the alternatively spliced exon v3 sequence are modified by heparan-sulphate (HS) side chains, which enable the binding to cytokines that have a HS-binding site, including HGF, and heparin-binding epidermal growth factor (HBEGF).[3,41,55,62] Under normal conditions, CD44 protein is almost undetectable in the kidney except for passenger leukocytes.[48] However its expression is markedly upregulated in inflammatory renal diseases, particularly in injured tubules, both in human diseases and in animal models.[4,12,47,52] Its expression on tubules closely correlates with inflammation, tubular damage and interstitial fibrosis in IgA nephropathy[12] and renal transplantation.[25,46] Previously, we showed in a murine model of chronic obstructive nephropathy that CD44-deficiency prevents renal fibrosis but aggravates tubular injury through lowering of both TGF-β1 and HGF antagonistic signaling pathways,[47] indicating that de novo expression of CD44 in injured kidneys contribute to fibrosis-development and also to TEC-survival.

In order to dissect the role of CD44-overexpression on proximal TEC upon renal injury and, specifically, the function of CD44s and CD44v3-v10 (CD44v3) tubular expression, we generated transgenic mice overexpressing either the CD44s or the CD44v3 gene specifically in renal proximal TEC and subjected them to unilateral ureteral obstruction (UUO). Herein, we hypothesize that overexpression of CD44v3 on tubules might prevent tubular injury and renal fibrosis.

Methods

Generation of transgenic mice

Transgene expression was driven by the γ-glutamyl transpeptidase type 1 (γGT-1) gene promoter. The rat γGT promoter was removed from the plasmid pG2.2rasT24 and cloned into the pFABP-CD44s and pFABP-CD44v3-v10 pBluescript plasmids, generating the plasmids γGT-CD44s and γGT-CD44v3-v10. Both final plasmids contain a rabbit β-globulin intron and the poly(A) sequence for the human globulin gene separated by the CD44 gene. The γGT-CD44 plasmids were digested with the restriction enzymes SalI and Xbal and the DNA fragments containing the transgene were microinjected into the pronucleus of two one-cell FVB/N embryos and implanted into hormone-treated FVB/N females. Three founders for each construct were used for backcrossing with C57BL6 mice ten times. Offspring-genotype was assessed by PCR-analysis of genomic DNA using the following primers: sense (se) 5'-gagctcatcacatcaggca (γGT promoter), antisense (as) 5'-gagggtccatggtgatac (rabbit β-globulin intron).

In vitro stimulation of primary TEC

Primary TEC from wild-type (WT), CD44s-, and CD44v3-transgenic mice (n=3) were isolated and cultured as previously described.[43] Stimulation with 1ng/ml rhTGF-β1, 50ng/ml rhHGF, or 10ng/ml rhBMP-7 (R&D Systems, Abingdon, UK) was preceded by semi-starvation in 0.5% FCS-RPMI medium for 2 hours.

In vivo experimental design

Left kidney UUO was performed in pathogen-free male wild-type C57BL6 mice and CD44s-, CD44v3-transgenic mice, 8 to 12 weeks of age (n=6-8 per group), as previously described.[43] Contralateral non-obstructed kidneys served as control. Mice were sacrificed by cardiac exsanguination at day 1, 3, 7 and 14 after surgery. The Institutional Animal Care and Use Committee approved all experiments.

Histology

Renal tissues were fixed in 10% formalin for 24 hours and embedded in paraffin. For immunohistochemistry stainings the following antibodies have been used: rat IgG2 anti-CD44 antibody (1:100, hybridoma IM7.8.1, ATCC, Livermore, CA), goat anti-Ki-67 (1:500, SDp6, Neomarkers), rabbit anti-active-caspase-3 (1:100, Cell Signaling, Beverly, MA), rabbit anti-osteopontin (R&D Systems), rat anti-F4/80 (1:500, Serotec, Oxford, UK), rabbit anti-CD3 (1:500, SP7, Thermo Scientific, Copenhagen, Denmark), mouse IgG2a anti-α-smooth muscle actin (1:800, α-SMA, 1A4, DAKO), rabbit anti-phospho-Smad-1 antibody (1:500, Santa Cruz Biotechnology, Santa Cruz, CA), rabbit anti-rat IgG (1:3000, DAKO), goat anti- mouse IgG2a-HRP (1:100, DAKO), PowerVision poly HRP-anti-rabbit IgG (1:2, ImmunoLogic, Duiven, The Netherlands). Hyaluronan (HA) was detected by biotinylated HA-binding protein (1:200, Calbiochem, Darmstadt, Germany) and Avidin Biotin Complex (ABC, DAKO). Slides were developed using HRP-labeled

secondary antibody (DAKO) and DAB (Sigma-Aldrich, Zwijndrecht, The Netherlands). Collagen I and III deposition was revealed by Picosirius Red staining. All histopathological scorings and quantifications of the immunohistochemistry stainings were assessed in the cortex and cortico-medullary area in ten to fifteen non-overlapping fields (x20 magnification) of stained renal sections and performed in a blinded fashion.[43,47] CD44 expression was quantified as a percentage of the positive proximal tubules on the total amount of proximal tubules and graded on a 0 to 5 point-scale: 0 = no expression; 1 = <10% of CD44+ tubules; 2 = 10% to 25% of positive tubules; 3 = 25 to 50% of positive tubules; 4 = 50% to 75% of positive tubules; 5 = >75% of tubules expressing CD44. Tubular damage was rated on periodic acid-Schiff Diastase (PAS-D) stained slides according to the following criteria: tubular dilatation, epithelial simplification, and interstitial expansions. Lesions were graded on a scale from 0 to 5: 0 = normal; 1 = very mild, involvement of less than 10% of the cortex; 2 = mild, involvement of 10% to 25% of the cortex; 3 = moderate, involvement of 25% to 50% of the cortex; 4 = severe, involvement of 50 to 75% of the cortex; 5 = extensive damage involving more than 75% of the cortex. Edema was graded on PAS-D stained renal sections on a 0 to 3 scale: 0 normal, 1 mild, 2 moderate, 3 severe edema formation. Proliferation and apoptosis were assessed by counting the number of tubular epithelial cells positive for Ki-67 and active-caspase-3, respectively. For quantification of the other stainings, ten to fifteen high-power field (x20) pictures of the cortex were taken per slide; the positive areas were measured with a computerized image analyzer (Image pro-plus, Mediacybernetics, Germany).

Kidney homogenate preparation and ELISA

Frozen kidneys were homogenized in lysis buffer (150mM NaCl, 15mM Tris, 1mM MgCl2 pH 7.4, 1mM CaCl2, 1% Triton) with addition of 1% protease inhibitor cocktail (P8340, Sigma). Specific ELISAs (R&D Systems, Abingdon, UK) were utilized to measure MCP-1, HGF, TGF-β1 in kidney homogenates.

Real time quantitative RT-PCR

Total RNA was extracted from 10 frozen sections (30μm thick) of UUO kidneys or from primary TEC with Trizol reagent (Invitrogen, Breda, The Netherlands). RNA was converted to cDNA by using oligo-dT primers. Quantitative real-time PCR (Q–PCR) was performed on a LightCycler® 480 System (Roche, Heidelberg, Germany) using LightCycler® 480 SYBR Green I Master mix (Roche). SYBR green dye intensity was analyzed with linear regression analysis. Gene-expression was normalized towards the housekeeping gene TATA-box binding protein (TBP). Amplified genes and primers sequences are as follows: TBP se 5'-caggagccaagagtgaagaac as 5'-ggaaataattctggctcatagctact, plasminogen activator inhibitor-1 (PAI-1) se 5'-aagtctttccgaccaagag as 5'-ctgagatgacaaaggctgtg, TGF-β1 se 5'-accaactagcttcagctccac as 5'-ggcaaggaccttgctgtactg, Collagen type I se 5'-acctaagggtaccgctgga as 5'-tccagcttctccatctttgc, α-SMA se 5'-tgtgatattgacatcaggaagg as 5'-ggcaatgatcttgatcttcat, Snail-1 se 5'-cttctctaggccctggct as 5'-agaatggcttctcaccagtg, c-Met se 5'-tgggccggcttaaccaagtgc as 5'-tgttcgagagagcaccacctgca, cyclooxigenase-2 (COX-2) se 5'-gatgctcttccgagctgtg

as 5'-ggattggaacagcaaggattt, CD44-pan se 5'-tccgaattagctggacactc as 5'-ccacaccttctcctactattgac, CD44s se 5'-ttctggaatctgaggtctcc as 5'-caccttggccaccagagatcg, CD44v3 se 5'-catcatcaatgcctgatcca as 5'-agtcaaataccaacccaacag, Claudin-2 se 5'-gtagccggagtcatcctttg as 5'-ggcctggtagccatcatagt, BMP-7 se 5'-ctggcaggactggatcat as 5'-gttgatgaagtgaaccagtgtc, MCP-1 se 5'-catccacgtgttggctca as 5'-gatcatcttgctggtgaatgagt, ID-3 se 5'-ttagccaggtggaaatcctg as 5'- agctgtctggatcgggagat, Smad-6 se 5'-ctcagatgccagcatgtctc as 5'- tggtcgtacaccgcatagag, ALK-3 se 5'-agccctacatcatggctgac as 5'- attc-ctccacgattcctcct, VE-cadherin se 5'-tcatcaaacccacgaagtcc as 5'-ggtctgtggcctcaatgtaga, Claudin-5 se 5'-actggaggagcgctttac as 5'-gttggcgaaccagcagag. All primers were manufactured by Biolegio (Nijmegen, The Netherlands).

Immunoblotting

Lysates were prepared from 15 frozen sections (30μm thick) or from primary TEC incubated at 4°C for 30 min in RIPA lysis buffer. Lysates (n=3-6 per group) were subjected to immunoblot analysis using antibodies rabbit anti-phospho Smad-2/3 (1:500, Santa Cruz Biotechnology), rabbit anti-PAI-1 (1:1000, homemade, kind gift by Prof. Roger Lijnen, Center for Molecular and Vascular Biology, KU Leuven, Belgium), rabbit anti-phospho-cMet (1:500, Abcam, Cambridge, UK), rabbit anti-phospho ERK1/2 (1:1000, Cell Signaling), rabbit anti-COX-2 (1:1000, Abcam), rabbit anti-c-Met (Santa Cruz Biotechnology), mouse IgG1 anti-Smad-2/3 (1:1000, BD Pharmigen), goat anti-BMP-7 (1:500, Santa Cruz Biotechnology) or rabbit anti-ID-3 (1:1000, Santa Cruz Biotechnology). HRP-conjugated secondary antibodies (1:1000, DAKO) were used, and HRP activity was visualized with ECL-reagent (Amersham Pharmacia Biotech, Roosendaal, The Netherlands). β-actin was used as loading control and detected by mouse IgG1 anti-β-actin (1:30000, Abcam). Densitometric quantification analysis was performed on imagines of scanned films using the image processing program ImageJ (National Institute of Health, US).

In Cell Western assays

Cells were seeded onto 96-well plates coated with poly-lysine (Sigma-Aldrich). After 24 hours of stimulation, cells were fixed in 4% paraformaldehyde-PBS, pemeabilized with 0.1% Triton X-100-PBS and incubated for 90 min in blocking solution before incubation with the primary antibodies rabbit anti-phospho-cMet (Abcam) or rabbit anti-cMet (Santa Cruz Biotechnology). Subsequently, cells were incubated with goat anti-rabbit IRDye 800 nm and DRAQ5®. Plates were scanned using the Odyssey Infrared Imager (LI-COR, Lincoln, NE). The integrated intensities of the protein signals were determined using the Odyssey software.

Data analysis

Statistical analysis was performed using Mann-Whitney U test and Student's t-test. Data are shown as mean and standard error of the mean (SEM) and $P < 0.05$ was considered to be significant.

Results

Generation of γGT-CD44s/v3 transgenic mice and mice phenotyping

In order to target proximal tubular cells and to avoid potential renal development malformations, transgene expression was set under the control of the 5' regulatory promoter region of γGT-1 gene. γGT-1 protein is exclusively expressed at high level by proximal TEC in the kidney and the γGT-1 gene is mainly expressed from 3 weeks after birth.[19] Transgenic mice were generated by microinjecting one-cell FVB/N zygotes with the γGT-CD44s or the γGT-CD44v3 transgene constructs. The offspring-genotype was identified by PCR analysis of toe genomic DNA (Figure 1A). CD44 protein expression was evaluated in kidneys, liver, lungs, spleen, bladder and heart from transgenic and wild-type animals. CD44 was absent in WT-kidneys except for passenger leukocytes. In the transgenic mice, its expression was restricted to basolateral membranes of proximal tubules (Figure 1B) and was absent in other organs except for leukocytes and resident stem cells in intestinal crypts (data not shown). Transgenic mice showed normal glomerular/tubular histology (Figure 1C), plasma urea/creatinine levels comparable to WT animals, and absence of proteinuria (data not shown). Total peripheral blood mononuclear cell counts and proportions of blood monocytes, lymphocytes, and granulocytes were comparable in WT and transgenic animals (data not shown).

Figure 1. Transgene expression in transgenic mice.

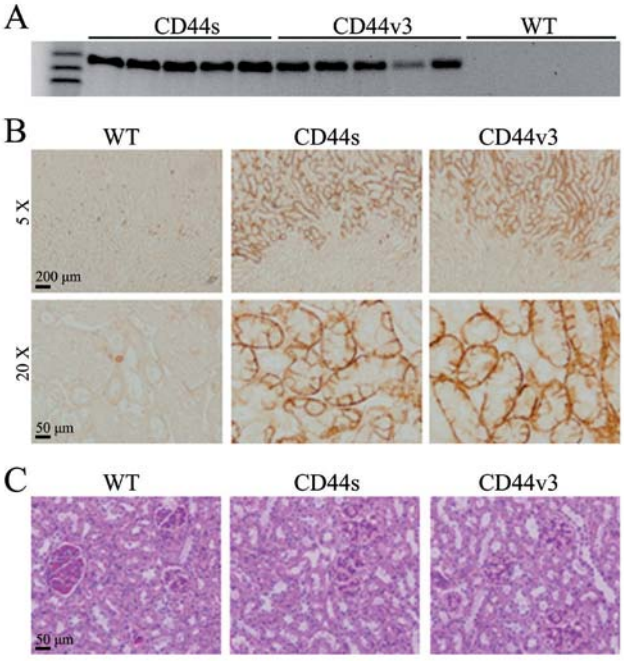

(A) Agarose gel electrophoresis. Transgenic construct detected in the genomic DNA of all transgenic mice and not in the DNA of wild-type animals. (B) Representative pictures of immunohistochemical staining for CD44-pan (x5, x20). (C) Renal morphology. Representative pictures of PAS-D stained renal sections of WT, CD44s and CD44v3 mice (x20).

Figure 2. In vitro assay with TEC isolated from three mice per strain.

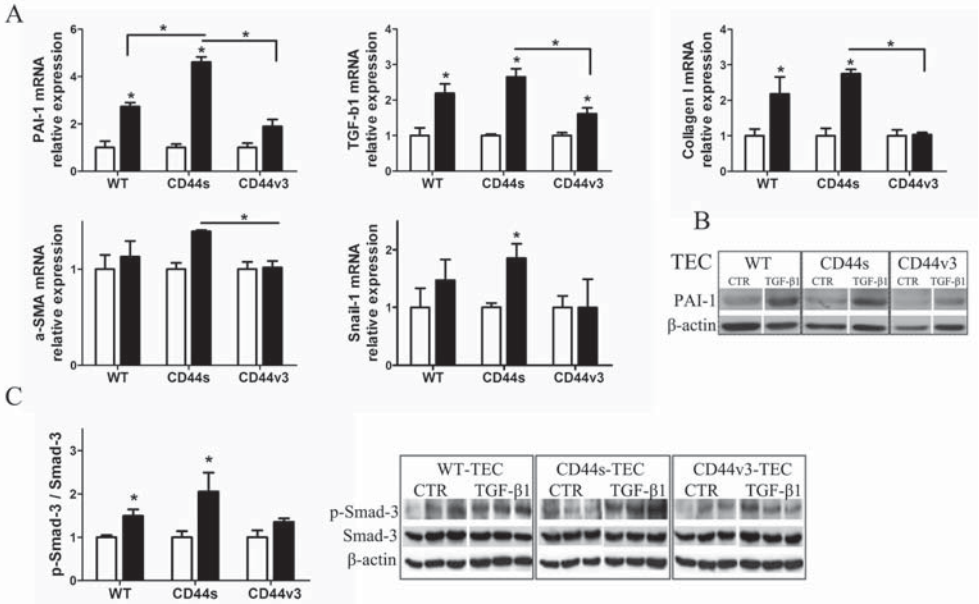

Cells were cultured with (black bars) or without (white bars) 1ng/ml hrTGF-β1 for 24 hours. (A) Quantitative real-time PCR for PAI-1, TGF-β1, collagen type I, and α-SMA genes. All values were corrected for the number of TBP transcripts. Mean +/- SEM, n=3, *:p<0.05. (B) Western-blot for PAI-1 and β-actin (loading control). (C) Western-blot analysis of the Smad-3 intracellular signaling pathways (ratio p-Smad-3/total Smad-3). β-actin was used as loading control. Data are presented as x-fold increase in comparison to the control unstimulated. Data expressed as mean +/- SEM, n=3, *:p<0.05.

Effects of CD44s/v3 overexpression by TEC on TGF-b1/HGF-induced cellularresponses in vitro

In our previous study, we determined that upon UUO CD44 is de novo expressed by TEC and its expression contributes to renal fibrosis, since CD44 knock-out mice displayed significantly less renal fibrosis after UUO. Furthermore, absence of CD44 impaired both TGF-β1 and HGF signaling in the UUO kidneys, indicating a role of CD44 isoforms in the activation of both pathways.
In order to characterize the role of CD44s and CD44v3 by proximal TEC in the pathogenesis of renal fibrosis, primary TEC isolated from WT, CD44s- and CD44v3-transgenic mice were stimulated with either TGF-β1 or HGF.
The gene expression, in response to TGF-β1, of pro-fibrotic mediators is shown in Figure 2A. TGF-β1-induced upregulation of the pro-fibrotic genes PAI-1, TGF-β1, collagen type I, and α-SMA was more pronounced in CD44s-overexpressing TEC and weaker/absent in CD44v3-TEC. Accordingly, CD44v3-TEC did not show an enhanced gene expression of the transcription factor Snail-1, which is known to trigger EMT.[50] As changes in mRNAs may not always translate in similar protein expression levels, we determined PAI-1 protein levels by Western-blot. The induction of PAI-1 protein expression, which is potently induced by TGFβ,[8] was much weaker in

Figure 3. In vitro assay with TEC isolated from three mice per strain.

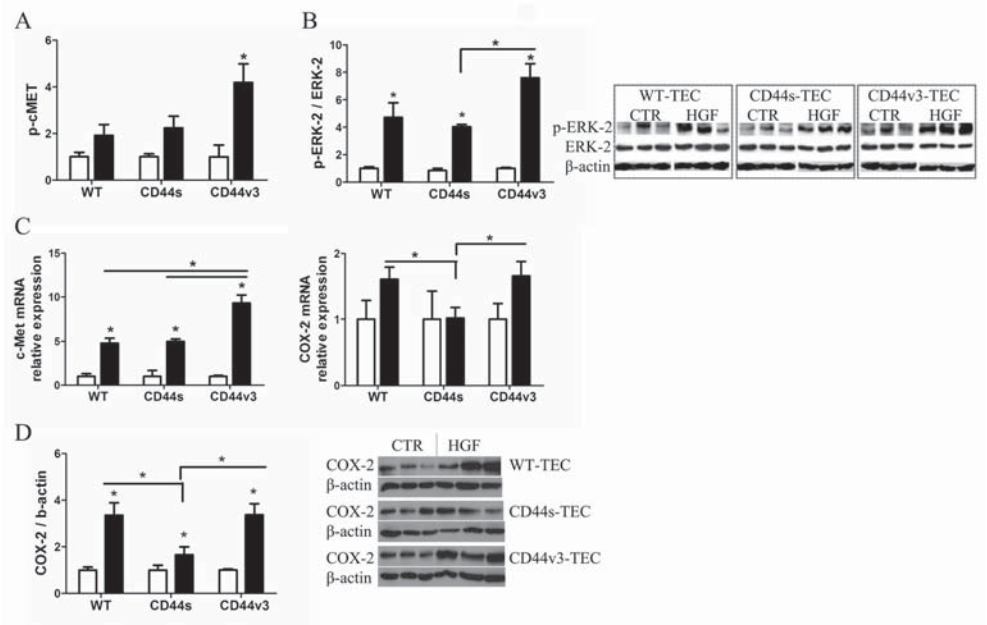

TEC were cultured for 24 hours with (black bars) or without (white bars) 50ng/ml hrHGF. (A) In Cell Western assay for phosphorylation rate of c-Met, values normalized for DRAQ5 stain. Mean +/- SEM, n=3, *:p<0.05. (B) Western-blot analysis of phosphorylation rate of ERK-2 (ratio p-ERK-2/total ERK-2). β-actin was used as loading control. Mean +/- SEM, n=3, *:p<0.05. (C) Analysis of c-Met and COX-2 gene expression by means of quantitative real-time PCR. Values were corrected for the number of TBP transcripts. Data are presented as x-fold increase in comparison to the control unstimulated. Bars show mean +/- SEM, n=3, *:p<0.05. (D) Western-blot analysis of COX-2. β-actin was used as loading control. Data are presented as x-fold increase in comparison to the control unstimulated. Bars show mean +/- SEM, n=3, *:p<0.05.

the CD44v3-overexpressing TEC than in the other cell-groups (Figure 2B). The phosphorylation of Smad-3, a key mediator of TGF-β1 signaling and transcription factor, was induced after TGF-β1-stimulation in WT and CD44s-TEC, and in a lower degree in CD44v3-TEC (Figure 2C).
On the contrary, in vitro stimulation with HGF led to an increased HGF intracellular pathway activation in CD44v3 overexpressing TEC in respect to WT and CD44s-TEC, as assessed by the phosphorylation rate of the HGF-receptor c-Met and of ERK-2, one of the HGF downstream signaling molecules[17] (Figure 3A,B). HGF stimulation greatly induced c-Met gene expression in CD44v3-TEC compared to WT and CD44s-TEC and resulted in higher mRNA levels of the anti-apoptotic cylooxygenase-2[22,34] in WT and CD44v3-TEC in respect to CD44s-TEC (Figure 3C). In agreement with the mRNA findings, COX-2 on protein level was induced by HGF and was more strongly upregulated in CD44v3-TEC than in CD44s-TEC (Figure 3D).
In conclusion, the in vitro data showed that overexpression of CD44v3 reduced TGF-β1 pathway

activation and enhanced HGF signaling in TEC, whereas TEC overexpressing CD44s were more sensitive to TGF-β1 pro-fibrotic actions. In order to translate these data to the in vivo situation, we compared the progression of obstructive nephropathy in WT, CD44s- and CD44v3-transgenic mice.

CD44 expression after UUO

Upon UUO, CD44 renal expression was upregulated in all mice and was predominantly localized at the basolateral membranes of tubular cells and on interstitial leukocytes (Figure 4A). In the WT obstructed kidneys CD44 strongly increased from day 1 to day 3 of UUO, reaching at day 7 almost the same level of expression as in the UUO kidneys of the transgenic mice (Figure 4B).

Figure 4. CD44 expression upon UUO.

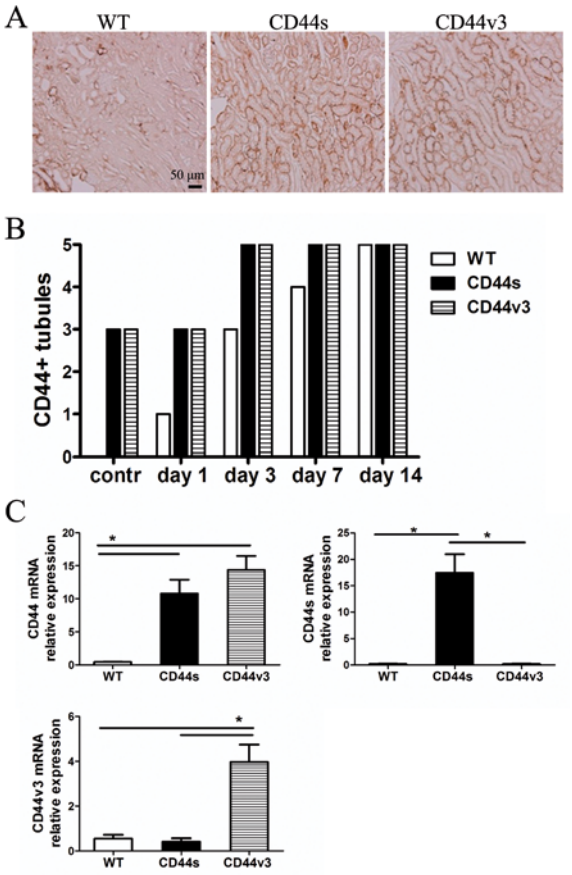

(A) Representative pictures of immunohistochemical staining for CD44 at day 1 after UUO (x10). (B) Semi-quantitative scoring of percentage of CD44-positive tubules in the cortex and cortico-medullary border region. Tubular expression of CD44 was graded on a 0 to 5-points scale. At each time-point the percentage-range of CD44+-positive tubules was equal among the kidneys from the same mouse-strain. Data expressed as mean, n=6-8, *:p<0.05. (C) Quantitative real-time PCR for CD44-pan, CD44s and CD44v3 at day 1 UUO. CD44 expression corrected for TBP. Bars show mean +/- SEM, n=6-8, *:p<0.05.

At day one, CD44 mRNA levels were only elevated in the transgenic kidneys, with a high CD44s and CD44v3 transcript levels only in the CD44s- and CD44v3-kidneys, respectively (Figure 4C).

Tubular damage after UUO

The semi-quantitative scoring of tubular injury revealed similar levels of tubular damage among the genotype groups from day 3. One day after surgery, the CD44s obstructed kidneys showed significantly severer tubular injury compared to the WT kidneys (Figure 5A). As tubular damage revealed significant differences among the mice strains at day one, we decided to focus our research on this early time-point, when the expression of the wild-type CD44 protein on renal tubules still differs from the CD44 transgene expression.

The pattern of tubular injury at early stage of UUO was not associated with differences in proliferation or apoptosis of TEC (data not shown). However, more interstitial edema was present in CD44s-kidneys compared to the WT and CD44v3-kidneys at day 1 of UUO (Figure 5B).

Figure 5. Tubular damage after UUO.

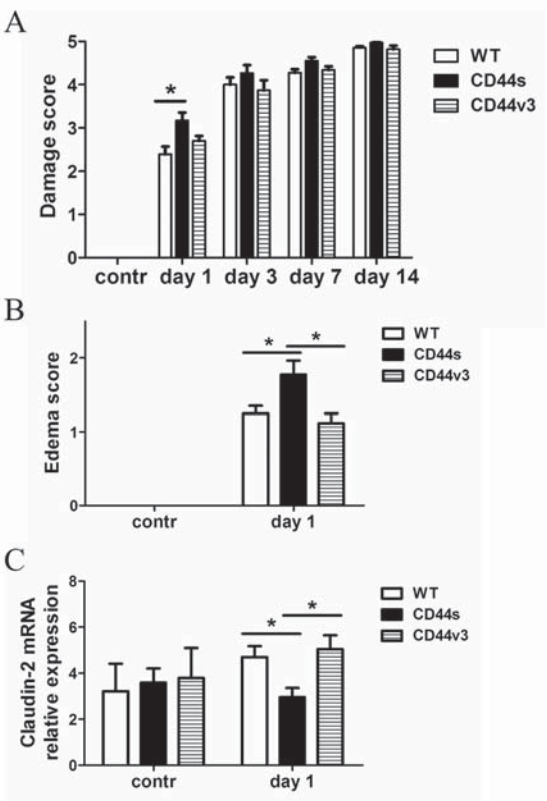

(A) Semi-quantitative scoring of tubular injury. Tubular damage was rated on a 0 to 5-points scale. Mean +/- SEM, n=6-8, *:p<0.05. (B) Semi-quantitative scoring of interstitial edema in contralateral and day 1-UUO kidneys. Scoring was set on a scale from to 0 to 3. Mean +/- SEM, n=6-8, *:p<0.05. (C) Quantitative real-time PCR for Claudin-2 in contralateral and day 1-UUO kidneys. Expression was corrected for TBP. Mean +/- SEM, n=6-8, *:p<0.05.

The increased edema at day 1 in CD44s-kidneys in comparison to the other strains was accompanied by a significantly lower gene expression of claudin-2, a tight-junction-associated adhesion molecule typical of the proximal tubules[45] (Figure 5C). Instead, the mRNA expression of VE-cadherin and claudin-5, two key components of adherens and tight endothelial junctions, respectively,[14] was found to be increased upon UUO at comparable levels among the mouse-groups (data not shown). Altogether these data indicate that upon obstruction variations in tubular injury degree among the strains are found solely when the WT CD44 gene (which is also present in the transgenic mice) is not yet highly expressed; the tissue damage in CD44s-kidneys was not due to an apoptosis/proliferation imbalance and was accompanied by more interstitial edema and diminished gene expression of the proximal TEC-adhesion molecule claudin-2.

Figure 6. Myofibroblasts accumulation, TGF-β1 synthesis and pathway activation.

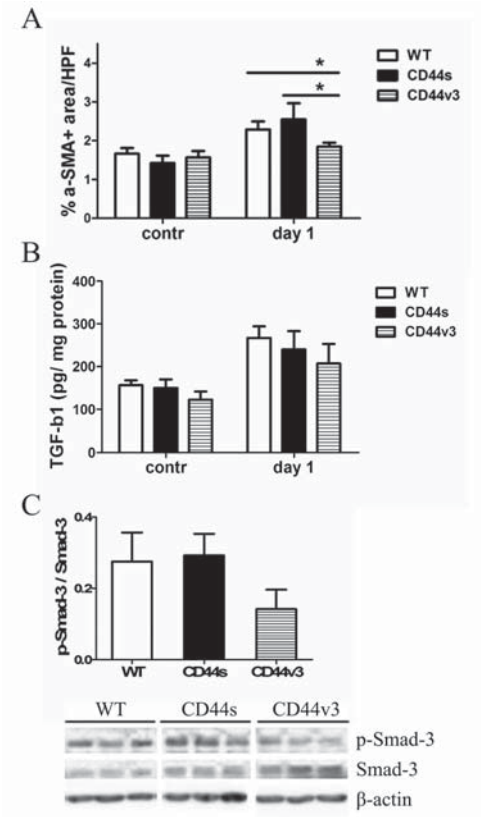

(A) α-SMA immunohistochemical staining for myofibroblast detection. The graph shows the percentage of positive renal cortical areas detected by the image analyzer. Mean +/- SEM, n=6-8, *:p<0.05. (B) TGF-β1 protein levels in renal homogenates. Amount of active TGF-β1 was determined by ELISA and corrected for amount of total proteins. Mean +/- SEM, n=6-8, *:p<0.05. (C) TGF-β1 signaling. Western-blot analysis of phosphorylated and total Smad-3 at day 1 UUO; β-actin was used as loading control. Mean +/- SEM, n=4, *:p<0.05.

Accumulation of CD44-ligands and inflammatory infiltrate after UUO

Since hyaluronan acid and osteopontin represent CD44 main ligands, are produced by TEC upon mechanical injury and promote inflammation,[1,44] their expression was determined by immunohistochemistry. Both ligands greatly accumulated at day 1 after UUO at similar levels among the genotype-groups (data not shown). Inflammation in obstructive nephropathy is characterized by recruitment of macrophages and T lymphocytes[16] that infiltrated the kidney parenchyma similarly in all mice groups (data not shown). Hence, TEC-overexpression of specific CD44 isoforms affected neither the degree of CD44-ligands accumulation nor the inflammatory cell influx in the UUO kidneys.

Myofibroblasts accumulation and pro/anti-fibrotic cytokines upon UUO

A pivotal role in fibrosis development is played by myofibroblast accumulation, which was found to be less in CD44v3-kidneys at day 1 after UUO in respect to WT and CD44s-kidneys (Figure 6A). Nevertheless, collagen deposition was similar in all groups (data not shown).

The balance between pro- and anti-fibrotic mediators is a major determinant of renal outcome in CKD.[13] Therefore, the levels of TGF-β1, HGF and BMP-7 were measured in UUO kidneys. No significant differences were observed in TGF-β1 renal levels among the mice strains (Figure 6B). After one day of obstruction, when TGF-β1 levels increased, CD44v3-kidneys showed a trend towards less TGF-β1 signaling activation (Figure 6C). At day 1 UUO CD44v3-kidneys displayed lower HGF levels as compared to WT (Figure 7A). Nevertheless the ability to activate the HGF-receptor, c-Met, was not impaired in the CD44v3-UUO kidneys (Figure 7B,C) as shown by western-blot analysis of phosphorylated and total c-Met in day 1-obstructed kidneys. This might suggest that when CD44v3 is overexpressed less HGF is required to properly activate its intracellular pathway.

BMP-7 is another anti-fibrotic molecule, which signals intracellularly through Smad-1, -5, and -8 and inhibits TGF-β1 signaling .[29,31] Upon one day of obstruction, the CD44v3-kidneys displayed more BMP-7 gene transcripts in respect to the other strains (Figure 8A). This increase in gene expression was accompanied by more BMP-7 protein expression (Figure 8B) and higher rate of phosphorylated Smad-1 proteins at day 1 of UUO in comparison to WT and CD44s-kidneys, respectively (Figure 8C). Moreover, after one day UUO the CD44v3-kidneys displayed lower levels of MCP-1, which can be downregulated by BMP-7 (Figure 8D).[15]

Effects of CD44s/v3 expression by TEC in response to BMP-7 in vitro

To further explore the contribution of CD44v3 tubular expression in the cellular response to BMP-7, primary TEC from wild-type and transgenic mice were stimulated with BMP-7. Overexpression of CD44s or CD44v3 had opposite effects in the BMP-7-induced changes in mRNA levels in TEC. Overexpression on TEC of CD44s resulted in unchanged levels of several mRNAs, whereas overexpression of CD44v3 induced a strong downregulation in MCP-1 gene expression and a higher expression of the BMP-7 target genes ID-3, Smad-6 and ALK-3 (BMP-7 receptor

Figure 7. HGF levels and signaling.

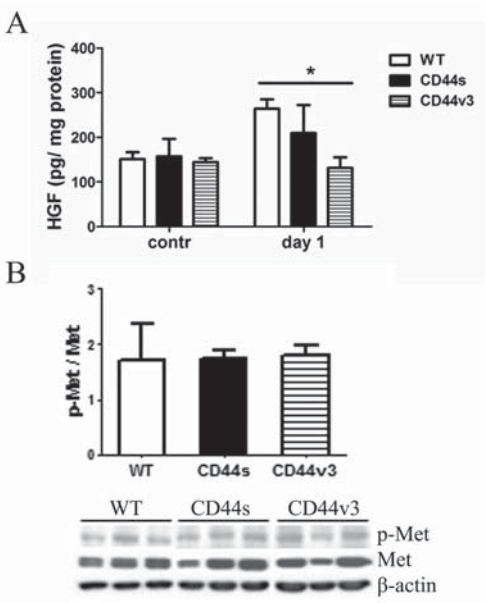

(A) HGF levels in renal homogenates, measured by ELISA, and normalized for the total protein amount. Mean +/- SEM, n=6-8, *:p<0.05. (B) HGF signaling pathway. Western-blot analysis of phosphorylated and total c-Met receptor at day 1 UUO. β-actin was used as control. Mean +/- SEM, n=3, *:p<0.05.

Figure 8. BMP-7 levels and signaling.

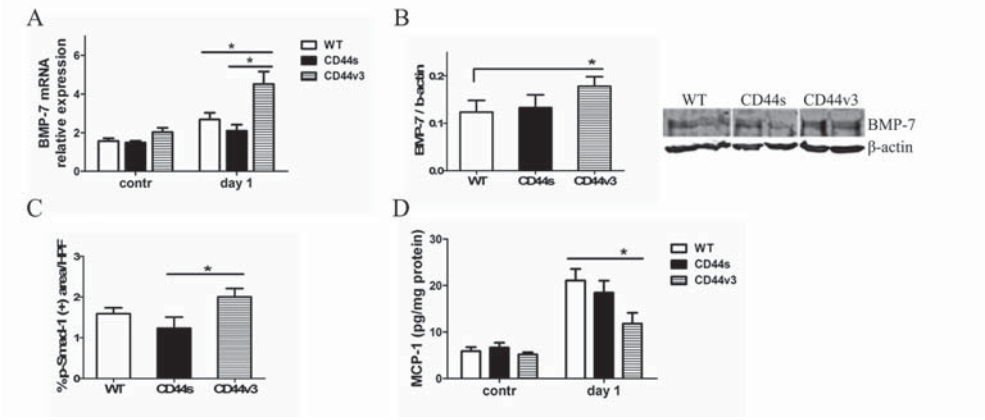

(A) Quantitative real-time PCR for BMP-7. Results were normalized for the number of TBP transcripts. Mean +/- SEM, n=6-8, *:p<0.05. (B) BMP-7 protein levels in UUO day 1. Protein amount quantified by western-blot and normalized for β-actin. Mean +/- SEM, n=7, *:p<0.05. (C) BMP-7 signaling in UUO day 1. Quantification of immunohistochemical staining for phospho-Smad-1, results expressed in percentage of the total analyzed renal area. Mean +/- SEM, n=6-8, *:p<0.05. (D) MCP-1 levels. Renal MCP-1 levels were determined by ELISA and corrected for the total protein amount. Mean +/- SEM, n=6-8, *:p<0.05.

type I)[15,28] as compared to stimulated CD44s-TEC (Figure 9A). In addition, the protein levels of ID-3 after BMP-7-stimulation displayed a greater increase in expression in CD44v3-TEC than in CD44s-TEC (Figure 9B).

Figure 9. In vitro stimulation of TEC with (black bars) or without (white bars) 10ng/ml hrBMP-7 for 24 hours.

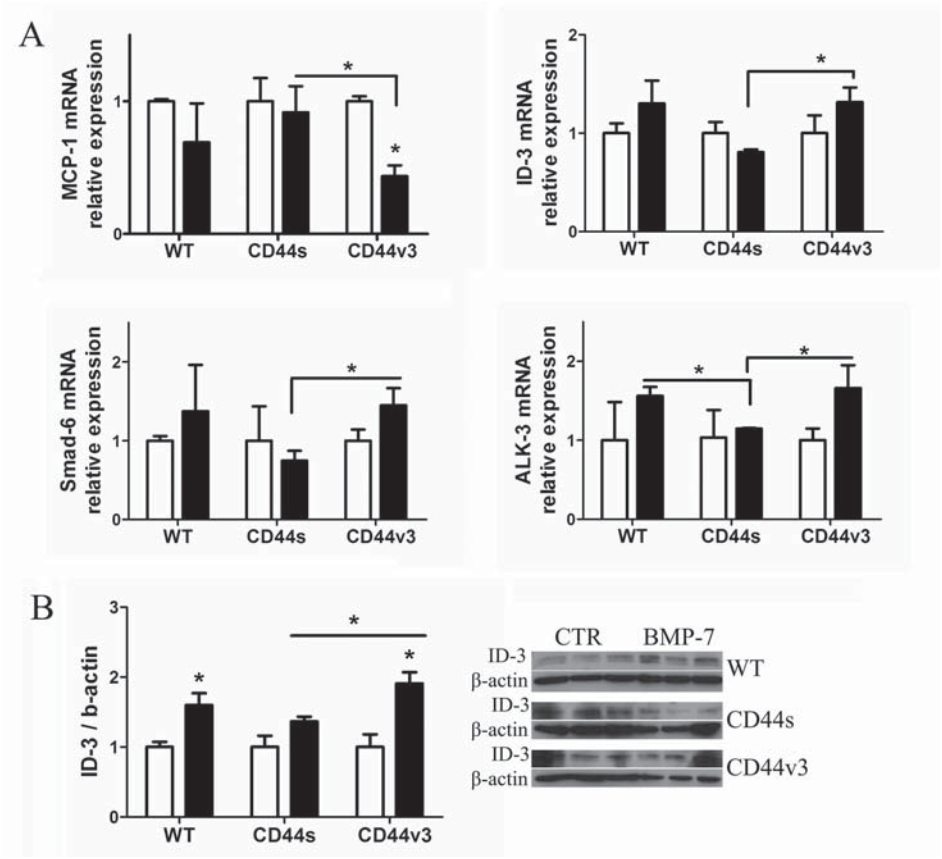

Cells were isolated from three mice per strain. (A) Quantitative real-time PCR for BMP-7 target genes (MCP-1, ID-3, Smad-6, ALK-3). All values were corrected for the number of TBP transcripts. Data are presented as x-fold increase in comparison to the control, equal to 1. Bars show mean +/- SEM, n=3, *:p<0.05. (B) Western-blot analysis of ID-3. β-actin was used as control. Data are presented as x-fold increase relative to the control, equal to 1. Mean +/- SEM, n=3, *:p<0.05.

Discussion

Decline in renal function and progression to end-stage renal failure are strongly predicted by the degree of tubulointerstitial inflammation and fibrosis.[2] Therefore, insight into the mechanisms initiating tubulointerstitial lesions, inflammation, and fibrosis is fundamental for the development of therapeutic strategies for prevention or treatment of progressive kidney diseases.

Although, we previously demonstrated that CD44 expression on tubules correlates with tubular damage degree, and is involved in renal fibrosis development,[25,47] the role of specific CD44 isoform in the pathogenesis of CKD remains undiscovered. Therefore, the present study aimed to clarify the function of two CD44 isoforms, CD44s and CD44v3, which are found to be upregulated in the murine UUO model.

In the first in vitro experiments (Figures 2,3) we tested the hypothesis that an up-regulation of CD44v3 by TEC would favorite the response of cells to HGF and protect them from the fibrotic actions of TGF-β1, while a high expression of the CD44 standard isoform in these cells would have the opposite effects. Primary TEC induced a more pronounced pro-fibrogenic response upon TGF-β1 stimulation when CD44s was highly expressed, whereas, CD44v3-TEC presented a much weaker response to TGF-β1 in term of gene expression, induction of PAI-1 protein and phosphorylation of Smad-3, which mediates TGF-β1-signaling and once in the nucleus directly binds to CAGA boxes sequences within the promoter of the PAI-1 gene[8] (Figure 2). Interestingly, only CD44s-TEC showed upregulated gene expression of α-SMA, a myofibroblasts marker, and Snail-1, an EMT transcription factor. The latter is found activated in patients with renal fibrosis, and its activation is sufficient to trigger kidney fibrosis in mice.[6,60]

CD44 can interact with TGF-β receptor type I and the binding of HA to CD44 stimulates TGF-β receptor type I serine/threonine kinase activity which, in turn, increases Smad2/3 phosphorylation.[5] All CD44 isoforms share an N-terminal cartilage link protein homology domain that constitutes the hyaluronan-binding site; however, the HA-binding affinity is regulated by a complex of modifications, involving alternative splicing and posttranslational modifications.[54] For instance, addition of heparan sulphate,[18] keratin sulphate[53] and chondroitin sulphate[7] decrease affinity for HA due to their negative charge. The results obtained from in vitro stimulation with TGF-β1 might be explained by a low HA-binding affinity of CD44v3 in respect to CD44s which, in turn, results in a weaker activation of the TGF-β receptor type I.

When HGF was added to tubular cells, CD44v3-TEC showed a higher phosphorylation rate of c-Met and ERK-2 and a greater c-Met gene expression in comparison to WT- and CD44s-TEC (Figure 3). Gene and protein expression of COX-2, which is HGF-inducible,[27] remained significantly lower upon HGF-stimulation in the TEC overexpressing CD44s. Besides its role in cell growth,[27] COX-2 has been implicated in abnormal fibrotic repair,[24,56] and in modulating HGF-driven action against TGF-β1-induced myofibroblast transdifferentiation and collagen I production.[26,65] Our in vitro data confirm previous studies, in which a physical and functional interaction between CD44v3 and HGF was shown. The HGF-binding to CD44v3 leads to phosphorylation of c-Met and activation of the MAP kinases ERK-1 and -2 in a heparin sulphate-dependent fashion.[55] Other

studies demonstrated that the CD44v6 isoform can also function as co-receptor for the c-Met,[38] but presumably the CD44-variant 3 is capable of concentrating HGF through the binding to its HS chains before presenting them to their receptor. In conclusion, the present in vitro data show that CD44v3 overexpressing TEC display less profibrotic TGF-β1 signaling and more antifibrotic HGF-signaling upon TGF-β1 and HGF stimulation, respectively. We therefore hypothesized that CD44v3 overexpression on TEC might diminish tubular damage and renal fibrosis in vivo during chronic obstructive nephropathy.

We determined that the degree of tubular injury was comparable among the mouse-genotypes at late time-points, whereas tubular damage was more severe in CD44s-kidneys after one day of obstruction (Figure 5). The similar levels of renal damage among the mice strains are probably due to similar expression levels of CD44 by tubules in all groups at late time-points (Figure 4). Moreover, it has to be kept in mind that the transgenes are overexpressed only in a unique cell-type on a WT-background. Thus, overexpression of the WT CD44 gene upon injury by several renal cell-types and by hematopoietic cells might overwhelm the transgene function in the proximal tubules. The increased renal injury in mice overexpressing the CD44s transgene was associated with more interstitial edema and less Claudin-2 mRNA expression compared to the other strains (Figure 5). Gene expression of the endothelial junction proteins VE-cadherin and claudin-5 was similar in all groups (data not shown), suggesting that the appearance of edema is more likely due to disruption and, therefore, leakiness of the tubular epithelium rather than to a leaky renal endothelium. However, these findings need to be further studied at protein level. Claudin-2 belongs to the claudin family of tight-junction associated-proteins, which fine-tune the para-cellular transport in the nephrons.[11] There are no studies so far that examine claudins expression in obstructive nephropathy models. However, Medici et al. demonstrated that TGF-β1 exposure to a renal cell line induced loss of claudin-2 and other tight-junction proteins in a Smad-independent mechanism.[30] Thus, the loss in claudin-2 mRNA expression by CD44s-TEC could result from a more pronounced response to TGF-β1 and, possibly, lead to loss of cell polarity and epithelial barrier, herein, facilitating the rise of edema and tubular damage.

Overexpression of CD44s/CD44v3 by TEC did not affect the interstitial accumulation of CD44 major ligands, HA and osteopontin, which were highly expressed in the obstructed kidneys in similar amount among the mice strains (data not shown). Both ligands play an important role in renal inflammation: osteopontin mediates renal interstitial macrophage recruitment[37,40] and HA is crucial for leukocytes adhesion, extravasation and migration.[20,57] Indeed, the influx of macrophages and lymphocytes in the UUO kidneys correlated with CD44 ligands interstitial accumulation at day one (data not shown).

Myofibroblast differentiation and activation by TGF-β1 is a critical event in the pathogenesis of chronic kidney diseases. In our study, the overexpression of CD44v3 by TEC resulted in less accumulation of myofibroblasts in comparison to WT and CD44s-kidneys at day 1 after UUO (Figure 6). The in vivo results correlate with the in vitro findings, in which we showed that CD44v3-TEC were less responsive to TGF-β1 stimulation.

HGF and BMP-7 are found to be downregulated in later stages of CKD[33,64] and described by many as potential reno-protective and anti-fibrotic agents for CKD-treatment.[9] Lower levels of HGF were detected in obstructed CD44v3-kidneys in respect to WT and CD44s-kidneys. Nevertheless, the reduced amount of HGF did not impair the ability to activate the c-Met receptor (Figure 7). As previously shown,[46] CD44v3 can interact with HGF through its HS motives, therefore an overexpression of CD44v3 enhances cell responsiveness to HGF and less HGF is needed to activate the downstream-pathway in the CD44v3-kidneys.
BMP-7 can counterbalance the pro-fibrotic effects of TGF-β1 via inhibiting Smad-3-nuclear translocation[32] and increasing SnoN expression.[29] It was also shown to reduce damage in animal models of acute and chronic kidney injury, and suppress expression of cytokines/chemokines including MCP-1.[15] Our in vivo model revealed a higher synthesis of BMP-7 and a lower production of MCP-1 in the CD44v3-ligated kidneys (Figure 8). In osteoblastic cells BMP-7 was shown to bind cell surface heparan sulfates and this interaction was required for BMP-7 signaling.[21] In addition, Richard S. Peterson et al. demonstrated that Smad-1 interacts with the cytoplasmic domain of CD44.[41] In our study, BMP-7 led to a strong downregulation in MCP-1 mRNA levels only in CD44v3-TEC (Figure 9), and the induction of BMP-7 target genes ID-3, Smad-6, and ALK-3[28] was greater in CD44v3-TEC than in CD44s-TEC. Western-blot analysis of ID-3 showed a good agreement with the mRNA findings on protein level. Taken together, the in vivo and in vitro data indicate that the presence of CD44v3 on TEC may contribute to the cell response to BMP-7. Thus, we could wonder if CD44v3, which has HS chains, is the CD44-variant responsible for the BMP-7 and Smad-1 interaction.
Taken together, the present data suggest that CD44v3 decreases tubular injury and myofibroblast accumulation in the early stage of chronic obstructive nephropathy through downregulation of TGF-β1 pro-fibrotic signaling and interactions with HGF and presumably BMP-7.

Acknowledgements

The authors thank M.W.Lieberman (Pathology Dept., Baylor College of Medicine, Texas, USA) for kindly providing the pG2.2rasT24 plasmid and R. van der Neut (NIN, Amsterdam) for providing the pFABP-CD44s and pFABP-CD44v3-v10 pBluescript plasmids.

Grants

This work was supported by the Dutch Kidney Foundation, grant C08-2261.

Disclosures

No potential conflicts of interest were disclosed.

Author contributions

S.F., J.C.L., K.R. and E.R. conceived the study design and were involved in writing and reviewing the manuscript. E.R., G.J.D.T. and N.C. carried out experiments, analyzed and interpreted the data. All authors gave input into the final manuscript.

References

1. Asselman M, Verhulst A, Van Ballegooijen ES, Bangma CH, Verkoelen CF, De Broe ME. Hyaluronan is apically secreted and expressed by proliferating or regenerating renal tubular cells. Kidney Int 68: 71-83, 2005.
2. Becker GJ, Hewitson TD. The role of tubulointerstitial injury in chronic renal failure. Curr Opin Nephrol Hypertens 9: 133-138, 2000.
3. Bennett KL, Jackson DG, Simon JC, Tanczos E, Peach R, Modrell B, Stamenkovic I, Plowman G, Aruffo A. CD44 isoforms containing exon V3 are responsible for the presentation of heparin-binding growth factor. J Cell Biol 128: 687-698, 1995.
4. Benz PS, Fan X, Wuthrich RP. Enhanced tubular epithelial CD44 expression in MRL-lpr lupus nephritis. Kidney Int 50: 156-163, 1996.
5. Bourguignon LY, Singleton PA, Zhu H, Zhou B. Hyaluronan promotes signaling interaction between CD44 and the transforming growth factor beta receptor I in metastatic breast tumor cells. J Biol Chem 277: 39703-39712, 2002.
6. Boutet A, De Frutos CA, Maxwell PH, Mayol MJ, Romero J, Nieto MA. Snail activation disrupts tissue homeostasis and induces fibrosis in the adult kidney. Embo J 25: 5603-5613, 2006.
7. Chiu RK, Droll A, Dougherty ST, Carpenito C, Cooper DL, Dougherty GJ. Alternatively spliced CD44 isoforms containing exon v10 promote cellular adhesion through the recognition of chondroitin sulfate-modified CD44. Exp Cell Res 248: 314-321, 1999.
8. Dennler S, Itoh S, Vivien D, ten Dijke P, Huet S, Gauthier JM: Direct binding of Smad3 and Smad4 to critical TGF beta-inducible elements in the promoter of human plasminogen activator inhibitor-type 1 gene. EMBO J 17(11):3091-100, 1998.
9. Djamali A, Samaniego M: Fibrogenesis in kidney transplantation: potential targets for prevention and therapy. Transplantation 88: 1149-1156, 2009.
10. Dworkin LD, Gong R, Tolbert E, Centracchio J, Yano N, Zanabli AR, Esparza A, Rifai A. Hepatocyte growth factor ameliorates progression of interstitial fibrosis in rats with established renal injury. Kidney Int 65: 409-419, 2004.
11. Enck AH, Berger UV, Yu AS. Claudin-2 is selectively expressed in proximal nephron in mouse kidney. Am J Physiol Renal Physiol 281: F966-974, 2001.
12. Florquin S, Nunziata R, Claessen N, van den Berg FM, Pals ST, Weening JJ. CD44 expression in IgA nephropathy. Am J Kidney Dis 39: 407-414, 2002.
13. Florquin S, Rouschop KM. Reciprocal functions of hepatocyte growth factor and transforming growth factor-beta1 in the progression of renal diseases: a role for CD44?. Kidney Int Suppl 86: S15-20, 2003.
14. Gavard J, Gutkind JS. VE-cadherin and claudin-5: it takes two to tango. Nat Cell Biol 10: 883-885, 2008.
15. Gould SE, Day M, Jones SS, Dorai H. BMP-7 regulates chemokine, cytokine, and hemodynamic gene expression in proximal tubule cells. Kidney Int 61: 51-60, 2002.
16. Grande MT, Perez-Barriocanal F, Lopez-Novoa JM. Role of inflammation in tubulo-interstitial damage associated to obstructive nephropathy. J Inflamm (Lond) 7: 19-32, 2010.
17. Graziani A, Gramaglia D, dalla Zonca P, Comoglio PM. Hepatocyte growth factor/scatter factor stimulates the Ras-guanine nucleotide exchanger. J Biol Chem 268: 9165-9168, 1993.

18. Jackson DG, Bell JI, Dickinson R, Timans J, Shields J, Whittle N. Proteoglycan forms of the lymphocyte homing receptor CD44 are alternatively spliced variants containing the v3 exon. J Cell Biol 128: 673-685, 1995.

19. Jacquemin E, Bulle F, Bernaudin JF, Wellman M, Hugon RN, Guellaen G, Hadchouel M. Pattern of expression of gamma-glutamyl transpeptidase in rat liver and kidney during development: study by immunochemistry and in situ hybridization. J Pediatr Gastroenterol Nutr 11: 89-95, 1990.

20. Jiang D, Liang J, Noble PW. Hyaluronan as an immune regulator in human diseases. Physiol Rev 91: 221-264, 2011.

21. Irie A, Habuchi H, Kimata K, Sanai Y. Heparan sulfate is required for bone morphogenetic protein-7 signaling. Biochem Biophys Res Commun 308: 858-86, 2003.

22. Ishaque A, Dunn MJ, Sorokin A. Cyclooxygenase-2 inhibits tumor necrosis factor alpha-mediated apoptosis in renal glomerular mesangial cells. J Biol Chem 278: 10629-10640, 2003.

23. Iwano M, Plieth D, Danoff TM, Xue C, Okada H, Neilson EG. Evidence that fibroblasts derive from epithelium during tissue fibrosis. J Clin Invest 110: 341-350, 2002.

24. Keerthisingam CB, Jenkins RG, Harrison NK, Hernandez-Rodriguez NA, Booth H, Laurent GJ, Hart SL, Foster ML, McAnulty RJ. Cyclooxygenase-2 deficiency results in a loss of the anti-proliferative response to transforming growth factor-beta in human fibrotic lung fibroblasts and promotes bleomycin-induced pulmonary fibrosis in mice. Am J Pathol 158: 1411-1422, 2001.

25. Kers J, Xu-Dubois YC, Rondeau E, Claessen N, Idu MM, Roelofs JJ, Bemelman FJ, ten Berge IJ, Florquin S. Intragraft tubular vimentin and CD44 expression correlate with long-term renal allograft function and interstitial fibrosis and tubular atrophy. Transplantation 90: 502-509, 2010.

26. Kolodsick JE, Peters-Golden M, Larios J, Toews GB, Thannickal VJ, Moore BB. Prostaglandin E2 inhibits fibroblast to myofibroblast transition via E. prostanoid receptor 2 signaling and cyclic adenosine monophosphate elevation. Am J Respir Cell Mol Biol 29: 537-544, 2003.

27. Lee YH, Suzuki YJ, Griffin AJ, Day RM. Hepatocyte growth factor regulates cyclooxygenase-2 expression via beta-catenin, Akt, and p42/p44 MAPK in human bronchial epithelial cells. Am J Physiol Lung Cell Mol Physiol 294: L778-786, 2008.

28. Leeuwis JW, Nguyen TQ, Chuva de Sousa Lopes SM, van der Giezen DM, van der Ven K, Rouw PJ, Offerhaus GJ, Mummery CL, Goldschmeding R. Direct visualization of Smad1/5/8-mediated transcriptional activity identifies podocytes and collecting ducts as major targets of BMP signalling in healthy and diseased kidneys. J Pathol 224: 121-132, 2011.

29. Luo DD, Phillips A, Fraser D. Bone morphogenetic protein-7 inhibits proximal tubular epithelial cell Smad3 signaling via increased SnoN expression. Am J Pathol 176: 1139-1147, 2010.

30. Medici D, Hay ED, Goodenough DA. Cooperation between snail and LEF-1 transcription factors is essential for TGF-beta1-induced epithelial-mesenchymal transition. Mol Biol Cell 17: 1871-1879, 2006.

31. Meng XM, Chung AC, Lan HY. Role of the TGF-beta/BMP-7/Smad pathways in renal diseases. Clin Sci (Lond) 124: 243-254, 2013.

32. Mitu G, Hirschberg R. Bone morphogenetic protein-7 (BMP7) in chronic kidney disease. Front Biosci 13: 4726-4739, 2008.

33. Mizuno S, Matsumoto K, Nakamura T. HGF as a renotrophic and anti-fibrotic regulator in chronic renal disease. Front Biosci 13: 7072-7086, 2008.

34. Moore AE, Greenhough A, Roberts HR, Hicks DJ, Patsos HA, Williams AC, Paraskeva C. HGF/Met signalling promotes PGE(2) biogenesis via regulation of COX-2 and 15-PGDH expression in colorectal cancer cells. Carcinogenesis 30: 1796-1804, 2009.

35. Moore BB, Paine R, 3rd, Christensen PJ, Moore TA, Sitterding S, Ngan R, Wilke CA, Kuziel WA, Toews GB. Protection from pulmonary fibrosis in the absence of CCR2 signaling. J Immunol 167: 4368-4377, 2001.

36. Okada H, Kalluri R. Cellular and molecular pathways that lead to progression and regression of renal fibrogenesis. Curr Mol Med 5: 467-474, 2005.

37. Ophascharoensuk V, Giachelli CM, Gordon K, Hughes J, Pichler R, Brown P, Liaw L, Schmidt R, Shankland SJ, Alpers CE, Couser WG, Johnson RJ. Obstructive uropathy in the mouse: role of osteopontin in interstitial fibrosis and apoptosis. Kidney Int 56: 571-580, 1999.

38. Orian-Rousseau V, Chen L, Sleeman JP, Herrlich P, Ponta H. CD44 is required for two consecutive steps in HGF/c-Met signaling. Genes Dev 16: 3074-3086, 2002.

39. Ortiz A, Ucero AC, Egido J. Unravelling fibrosis: two newcomers and an old foe. Nephrol Dial Transplant 25: 3492-3495, 2010.

40. Persy VP, Verhulst A, Ysebaert DK, De Greef KE, De Broe ME. Reduced postischemic macrophage infiltration and interstitial fibrosis in osteopontin knockout mice. Kidney Int 63: 543-553, 2003.

41. Peterson RS, Andhare RA, Rousche KT, Knudson W, Wang W, Grossfield JB, Thomas RO, Hollingsworth RE, Knudson CB. CD44 modulates Smad1 activation in the BMP-7 signaling pathway. J Cell Biol 166: 1081-1091, 2004.

42. Ponta H, Sherman L, Herrlich PA. CD44: from adhesion molecules to signalling regulators. Nat Rev Mol Cell Biol 4: 33-45, 2003.

43. Pulskens WP, Rampanelli E, Teske GJ, Butter LM, Claessen N, Luirink IK, van der Poll T, Florquin S, Leemans JC. TLR4 promotes fibrosis but attenuates tubular damage in progressive renal injury. J Am Soc Nephrol 21: 1299-1308, 2010.

44. Quinlan MR, Docherty NG, Watson RW, Fitzpatrick JM. Exploring mechanisms involved in renal tubular sensing of mechanical stretch following ureteric obstruction. Am J Physiol Renal Physiol 295: F1-F11, 2008.

45. Reyes JL, Lamas M, Martin D, del Carmen Namorado M, Islas S, Luna J, Tauc M, Gonzalez-Mariscal L. The renal segmental distribution of claudins changes with development. Kidney Int 62: 476-487, 2002.

46. Rouschop KM, Roelofs JJ, Sylva M, Rowshani AT, Ten Berge IJ, Weening JJ, Florquin S. Renal expression of CD44 correlates with acute renal allograft rejection. Kidney Int 70: 1127-1134, 2006.

47. Rouschop KM, Sewnath ME, Claessen N, Roelofs JJ, Hoedemaeker I, van der Neut R, Aten J, Pals ST, Weening JJ, Florquin S. CD44 deficiency increases tubular damage but reduces renal fibrosis in obstructive nephropathy. J Am Soc Nephrol 15: 674-686, 2004.

48. Roy-Chaudhury P, Khong TF, Williams JH, Haites NE, Wu B, Simpson JG, Power DA. CD44 in glomerulonephritis: expression in human renal biopsies, the Thy 1.1 model, and by cultured mesangial cells. Kidney Int 50: 272-281, 1996.

49. Sato M, Muragaki Y, Saika S, Roberts AB, Ooshima A. Targeted disruption of TGF-beta1/Smad3 signaling protects against renal tubulointerstitial fibrosis induced by unilateral ureteral obstruction. J Clin Invest 112: 1486-1494, 2003.

50. Scarpa M, Grillo AR, Brun P, Macchi V, Stefani A, Signori S, Buda A, Fabris P, Giordani MT, De Caro R, Palu G, Castagliuolo I, Martines D. Snail1 transcription factor is a critical mediator of hepatic stellate cell activation following hepatic injury. Am J Physiol Gastrointest Liver Physiol 300: G316-326, 2011.

51. Screaton GR, Bell MV, Jackson DG, Cornelis FB, Gerth U, Bell JI. Genomic structure of DNA encoding the lymphocyte homing receptor CD44 reveals at least 12 alternatively spliced exons. Proc Natl Acad Sci U S A 89: 12160-12164, 1992.

52. Sibalic V, Fan X, Loffing J, Wuthrich RP. Upregulated renal tubular CD44, hyaluronan, and osteopontin in kdkd mice with interstitial nephritis. Nephrol Dial Transplant 12: 1344-1353, 1997.

53. Takahashi K, Stamenkovic I, Cutler M, Dasgupta A, Tanabe KK. Keratan sulfate modification of CD44 modulates adhesion to hyaluronate. J Biol Chem 271: 9490-9496, 1996.

54. van der Voort R, Manten-Horst E, Smit L, Ostermann E, van den Berg F, Pals ST. Binding of cell-surface expressed CD44 to hyaluronate is dependent on splicing and cell type. Biochem Biophys Res Commun 214: 137-144, 1995.

55. van der Voort R, Taher TE, Wielenga VJ, Spaargaren M, Prevo R, Smit L, David G, Hartmann G, Gherardi E, Pals ST. Heparan sulfate-modified CD44 promotes hepatocyte growth factor/scatter factor-induced signal transduction through the receptor tyrosine kinase c-Met. J Biol Chem 274: 6499-6506, 1999.

56. Wilborn J, Crofford LJ, Burdick MD, Kunkel SL, Strieter RM, Peters-Golden M. Cultured lung fibroblasts isolated from patients with idiopathic pulmonary fibrosis have a diminished capacity to synthesize prostaglandin E2 and to express cyclooxygenase-2. J Clin Invest 95: 1861-1868, 1995.

57. Wuthrich RP. The proinflammatory role of hyaluronan-CD44 interactions in renal injury. Nephrol Dial Transplant 14: 2554-2556, 1999.

58. Wynn TA. Cellular and molecular mechanisms of fibrosis. 214: 199-210, 2008.

59. Yokoi H, Sugawara A, Mukoyama M, Mori K, Makino H, Suganami T, Nagae T, Yahata K, Fujinaga Y, Tanaka I, Nakao K. Role of connective tissue growth factor in profibrotic action of transforming growth factor-beta: a potential target for preventing renal fibrosis. Am J Kidney Dis 38: S134-138, 2001.

60. Yoshino J, Monkawa T, Tsuji M, Inukai M, Itoh H, Hayashi M. Snail1 is involved in the renal epithelial-mesenchymal transition. Biochem Biophys Res Commun 362: 63-68, 2007.

61. Yu Q, Stamenkovic I. Cell surface-localized matrix metalloproteinase-9 proteolytically activates TGF-beta and promotes tumor invasion and angiogenesis. Genes Dev 14: 163-176, 2000.

62. Yu WH, Woessner JF Jr, McNeish JD, Stamenkovic I. CD44 anchors the assembly of matrilysin/MMP-7 with heparin-binding epidermal growth factor precursor and ErbB4 and regulates female reproductive organ remodeling. Genes Dev 16: 307-323, 2002.

63. Zeisberg M, Hanai J, Sugimoto H, Mammoto T, Charytan D, Strutz F, Kalluri R. BMP-7 counteracts TGF-beta1-induced epithelial-to-mesenchymal transition and reverses chronic renal injury. Nat Med 9: 964-968, 2003.

64. Zeisberg M, Muller GA, Kalluri R. Are there endogenous molecules that protect kidneys from injury? The case for bone morphogenic protein-7 (BMP-7). Nephrol Dial Transplant 19: 759-761, 2004.

65. Zhang A, Wang MH, Dong Z, Yang T. Prostaglandin E2 is a potent inhibitor of epithelial-to-mesenchymal transition: interaction with hepatocyte growth factor. Am J Physiol Renal Physiol 291: F1323-1331, 2006.